Measurement of Resistivity at Low Temperatures

Robbie Ellis, Junseo Shin, and Daniel Rothstein[1]

[1]*Department of Physics, Washington University, St. Louis, Missouri 63130*

(Dated: May 20, 2025)

At low temperatures, materials can experience phenomena such as superconductivity and magnetic ordering. For Lead (Pb) and Niobium Titanium (NbTi), there is a critical temperature T_C where the characteristics of superconductivity appears [1][2]. For Copper, at low temperatures, the phonon contribution to the resistivity changes from a T scaling to a T^5 scaling, which can be described by the Bloch-Grüneisen formula [3]. Dysprosium is also known to transition from a paramagnetic state to a ferromagnetic state below 179 K, further highlighting the diversity of low-temperature behaviors in materials [4]. In this experiment, the temperature and resistivity of these materials are measured at low temperatures to re-evaluate the known properties of these materials described in the literature. Despite equipment limitations and fragmented data collection, examination of the recorded data displays the mentioned phenomena very clearly, which provides critical information to understand the properties of materials at low temperatures.

INTRODUCTION

In 1911, Dutch physicist Heike Onnes discovered a sudden disappearance of electrical resistance in solid Hg at a temperature of 4.2K with the use of liquid helium as a cooling agent [5]. This low resistance state, now referred to as a "superconducting" state, has been observed in several other materials, such as Pb, NbTi, and several other metals/metalic compounds. Around 20 years after Onnes' discovery, two German physicists, Walther Meissner and Robert Ochsenfeld discovered that a material in a superconducting state will prevent the formation of an internal magnetic field in the presence of an external magnetic field. This phenomenon, known as the Meissner effect, arises from the generation of surface currents which contribute a magnetic field essentially equal in magnitude and opposite in direction of the induced internal field [6]. These discoveries uncovered a few of the interesting and unpredictable ways in which matter behaves at low temperatures.

When considering properties of solids, it is necessary to consider how the lattice of nuclei interact with electrons in the material. While there are obvious Coulomb forces, there are also other interactions that electrons participate in. Vibrations in lattice elements will arise as a result of nuclei being moved slightly from equilibrium–this vibration is quantized, with quanta known as phonons. While these phonons are not real particles (unlike a photon, which would analogously be thought of as a quanta of a "vibration" in the electromagnetic field), they share many similar properties. For example, phonons couple to electrons as an actual particle (such as a photon) would. An important aspect of phonons is that they obey Bose-Einstein statistics, and are not conserved–this results in an equilibrium distribution analogous to that of photons:

$$f(E,T) = \frac{1}{e^{\frac{E}{T}} - 1} \tag{1}$$

considered in natural units, with $k = \hbar = c = 1$.

The more interesting aspects of phonons arise from the fact that there is a minimum wavelength, which can be seen to be twice the distance between adjacent points in the lattice (L). This minimum wavelength puts an upper bound on the possible energies a phonon can have, since $E = \frac{c_s}{2\pi\lambda}$ (where c_s is the speed of sound in the material), which can be seen as a generalization of the equation for photon energy (given in natural units). In materials where the distance between lattice points is the same in all dimensions, it is evident that the possible energy states are confined to a cube, with side lengths proportional to $\frac{1}{L}$. This cutoff makes the properties of the phonon population greatly temperature dependent, resulting in a number density proportional to T^3 at low temperatures, and T at high temperatures [6].

It can also be shown that at low temperatures, the number of scattering events that contribute to the resistivity of the material scales as T^2, while at higher temperatures phonons will have enough energy on average to make every collision contribute to resistivity–therefore, the phonon contribution to resistivity is predicted to be proportional to T^5 at lower temperatures, and T at higher temperatures [6].

These principles can be used to form a quantitative model for resistivity due to electron-phonon interactions, which is encapsulated by the Bloch–Grüneisen formula

$$\rho(T) = \rho_0 + 4\rho_\Theta \left(\frac{T}{\Theta}\right)^5 \int_0^{\frac{\Theta}{T}} \frac{u^5}{(e^u - 1)(1 - e^{-u})} \mathrm{d}u \tag{2}$$

where Θ, the Debye temperature, determines the temperature at which the transition from T^5 and T resistivity scaling occurs, and is given by $\frac{c_s}{4\pi}(\frac{6N}{\pi V})^{\frac{1}{3}}$, where N is the number of atoms in the material and V is it's volume [3]. ρ_Θ is a material-specific constant which describes the strength of the electron phonon coupling, and ρ_0, the residual resistivity, is the resistivity present at around 0 K. ρ_0 can also be used to calculate the materials residual resistivity ratio (RRR), a useful material constant describing the ratio of resistivities measured at 293 K

and 4.2 K. In most materials, the resistivity will be approximately constant below 4.2 K, in which case ρ_0 to be used for the materials resistivity at 4.2 K. In materials that superconduct, a RRR value cannot be assigned in the same way as a result of the resistivity dropping to 0 Ω·m. Instead, the resistivity just before the transition to superconductivity is used in place of ρ_0.

Some models of superconductivity (namely, the Bardeen-Cooper-Schrieffer theory) also attribute the phenomenon to electron-phonon coupling. At low enough temperatures, slight attraction between electrons due to electron-phonon coupling can result in the electrons forming a paired state (called a "Cooper pair"), which follows Bose-Einstein statistics. As a result, other electrons can form the same state, which results in a perfectly coherent state of Cooper pairs that are stable against disturbances that would normally cause resistivity, resulting in a current that experiences zero resistivity.

Another interesting phenomenon that occurs at lower temperatures is magnetic ordering–once the temperature falls below a certain threshold, materials that are paramagnetic at higher temperatures can undergo a phase transition and become ferromagnetic (or antiferromagnetic). In this state, electrons in the material stabilize themselves by aligning their spins to match (to be opposite of) their neighbors. This phase transition results in a noticeable, abrupt change in the resistivity of the material.

This experiment will highlight these phenomena in various materials. The voltages across samples of Pb and NbTi will be measured to infer resistivity, allowing the superconductivity transition temperature to be measured. The same process will also be applied to Cu and Dy to calculate its Debye temperature and RRR, and the temperature of magnetic ordering, respectively.

Methodology and Setup

Low Voltage Measurements In order to measure voltage across the samples effectively we used four-terminal sensing. In four-terminal sensing, separate pairs of wires handle the current supply and voltage measurement functions, which minimizes the resistances of the lead wires.

The two "source" wires supply a current I across the samples, while the two "sense" wires measure the voltage drop V directly across the sample without any additional voltage drop from the wires carrying current, as seen in Figure 1. This ensures that the measured voltage reflects only the drop over the sample itself instead of in the lead wires. The 4-wire sensing method is a fundamental procedure used to measure voltages for low temperature materials which is then used to measure the temperature and resistivity of the sample.

Using the sensitive voltage measurements across the sample, the resistivity can be determined by first calculating the resistance across each sample using Ohm's Law, $R = \frac{V}{I}$. Then the resistivity of a sample can be calculated using the formula

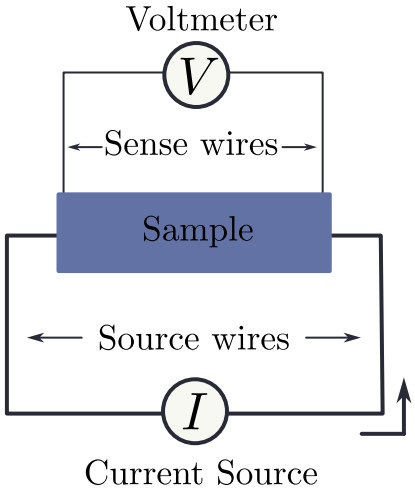

FIG. 1: A diagram of a four terminal sensing apparatus

$$\rho = R\frac{A}{L} \tag{3}$$

where A is the cross-sectional area of the sample and L is the length of the sample—i.e. Cu and NbTi wires have a circular cross sectional area $A = \pi r^2$ while Dy and Pb are thin foils with area $A = w \cdot t$. The values for current through these materials were 1 mA for Cu and NbTi, and 30 mA for Dy and Pb.

In order to measure the temperature of each sample, there is a similar resistor with a fixed relationship between resistance and temperature. Using Ohm's law, $V = IR$, the resistance can be found which has a known relationship to temperature. Then a Chebyshev polynomial (with coefficients provided by the Cernox manufacturer's manual) was used, which relates the log resistance to the log temperature [7],

$$\log_{10} T = \sum_i a_i \cos(iw \log_{10} R) + b_i \sin(iw \log_{10} R) \tag{4}$$

In addition, the Cernox thermometer recommends excitation currents of 100 μA for above 30 K, 10 μA for 30 $\rightarrow$ 2.5 K, and 1 μA for below 2.5 K to prevent the internal heating of the thermometer from affecting the temperature measurements.

To minimize heat transfer between the sample and the environment, the samples is housed in two dewars (double walled container): the inner dewar contains the sample and liquid helium (LHe) being sealed by a variable vacuum, while the outer dewar has an open top which is filled with liquid nitrogen and surrounded by a permanent vacuum jacket. Furthermore, there are three vacuum pumping systems in place to precisely control the

pressures of the inner vessel containing the sample and the variable vacuum as the sample is cooled to low temperatures.

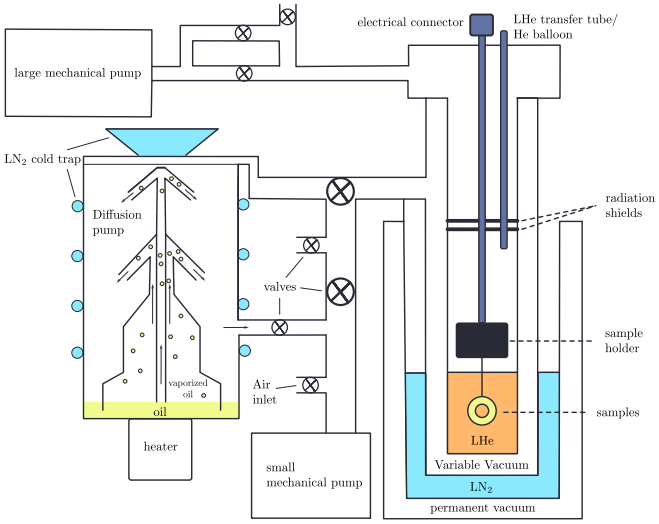

FIG. 2: Apparatus for Low Temperature Experiments.

Low Temperature Procedure Bringing a sample from room temperature ($\sim$ 300 K) to low temperatures down to $\sim$ 1 K requires three main cooling stages: First, the variable vacuum is set to roughly 5-10 Torr with the aid of the small mechanical pump to provide a good thermal connection between the inner and outer dewar. The samples were then cooled by filling the outer dewar with liquid nitrogen. Although this stage takes several hours to just cool the sample to $\sim$ 80 K, the cheap and abundant liquid nitrogen reduces the cost of cooling the sample with purely liquid helium, a much more expensive and rare resource.

After the sample has reached an equilibrium temperature in the LN_2 bath, the variable vacuum pressure must be decreased to $\sim 10^{-4}$ Torr to close the thermal connection between the inner and outer dewar prior to cooling the sample with liquid helium. This high vacuum must be attained using the diffusion pump which boils a special oil until it vaporizes and jettisons through a central column. As the vapor exits the column, the liquid nitrogen cold trap surrounding the walls of the pump quickly condenses the vapor back into a liquid which falls back down in the the reservoir to be reheated and vaporized again. The free molecular flow of the oil vapors create a jet stream which entrain other gas molecules through the central column and out the bottom of the pump which ultimately leads to the high vacuum for the variable vacuum.

Before the liquid helium is transferred via a pressure differential from the storage dewar to the inner dewar, the air inlet must be vented to prevent dangerous pressure build up in the inner dewar which could explode the apparatus. When the liquid helium is transferred, the sample is cooled very quickly to $\sim$ 4 K which does not allow the data acquisition software to precisely measure the temperature changes of the samples. To find these intermediate temperatures, the sample would be slowly lifted in order to allow for the sample to warm slowly. This step was unfortunately not done because of a lack of liquid Helium.

To get to $\sim$ 1 K, the large mechanical pump can be used to decrease the pressure of the inner dewar. Although Gay-Lussac's law $P \propto T$ might explain this transition, it is actually due to the vapor-liquid phase transition mediated at the surface of the liquid; when we lower the pressure in the dewar, the vapor pressure decreases, so the high energy helium molecules on the liquid surface evaporate out of the liquid which carry the heat energy along with it. This evaporation cools the remaining liquid lowering the temperature of the helium liquid and the samples submerged in it. Thus the analog pressure gauge used to monitor the pressure of the inner dewar measures the vapor pressure of the liquid helium which can be used to determine the temperature of the samples using lookup tables [8].

Due to data that was inconsistent with the conditions of the experiment, the thermometer had to be recalibrated. The voltage drop across the thermometer probe at room temperature corresponded to a temperature of 270 K based on (4). To correct for this clearly erroneous reading, a scaling factor of 0.9665 was applied to all computed resistances in order to have the resistance computed at room temperature correspond to room temperature.

Analysis

The uncertainty the dimension measurements of each material propagate into the resistivity calculation and are shown in Tables 1 and 2 for wire and film shaped materials, respectively.

Material	D (μm)	L (cm)	$\delta\rho/\rho$
NbTi	112 $\pm$ 4	10.0 $\pm$ 0.4	8%
Cu	165 $\pm$ 10	482.0 $\pm$ 0.5	10%

TABLE I: Dimensions (and their associated uncertainty) of wire-shaped material, with D corresponding to the cross-sectional diameter of the material, and L corresponding to length. The associated uncertainty of the resistivity is given as $\delta\rho/\rho$, calculated via use of (3). Uncertainty from the computed resistance is neglected.

Material	w (mm)	t (mm)	L (mm)	$\delta\rho/\rho$
Pb	1.6 ± 0.2	0.12 ± 0.01	17.0 ± 0.5	20%
Dy	2.7 ± 0.2	0.11 ± 0.01	18.0 ± 0.8	10%

TABLE II: Dimensions (and their associated uncertainty) of film-shaped material, wit w corresponding to materials width, t corresponding to thickness, and L corresponding to length. The associated uncertainty of the resistivity is given as $\delta\rho/\rho$, calculated via use of (3)

All resistivity in this section are given with the understanding that that the uncertainty corresponding to the material listed in Table I or II applies. The data presented in the following figures will use a subset of the recorded data for temperatures at which data is dense (below 3 K and above 40 K) in order to highlight trends without frequent overlapping.

The resistivity of Pb was determined from the measured voltages and use of (3). The resistivity at their corresponding temperatures are shown in Figure 3:

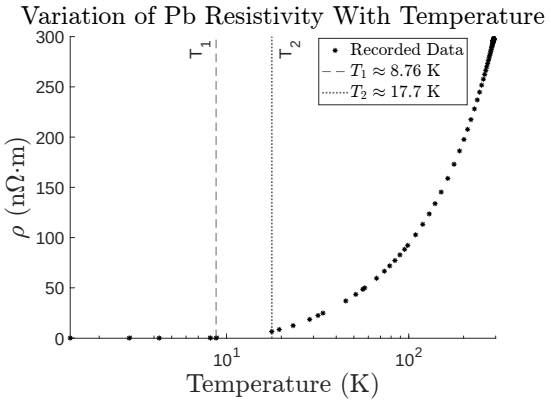

FIG. 3: Resistivity of lead as a function of temperature. Superconductivity is observed at temperatures measured below T_1, and transitions at a temperature between T_1 and T_2.

The resistivity of Pb is seen to drop to 0 Ω·m at $T_1 = 8.76$ K, with the next nonzero resistivity at $T_2 = 17.7$ K. Due to the lack of data points in this range, it is not possible to make a more precise estimate than $T_c = 13.2 \pm 4.5$ K. While the data above $T_2 = 17.7$ K in Figure 3 follows a linear trend, adherence to this trend cannot be justified within $T_1 < T < T_2$, therefore is not used to estimate T_c.

Plotting the resistivity of NbTi at different temperatures also showed a transition to superconductivity:

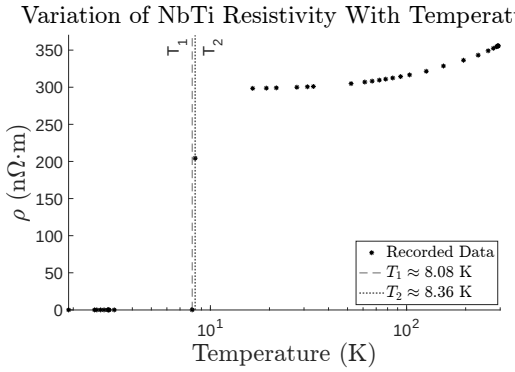

FIG. 4: Resistivity of NbTi as a function of temperature. Superconductivity is observed at temperatures measured below T_1, and transitions at a temperature between T_1 and T_2.

The first measured temperature at which the resistivity of NbTi drops to 0 Ω·m is seen at $T_1 = 8.08$ K, with the next nonzero resistivity value recorded at $T_2 = 8.36$ K. This indicates that $T_c = 8.22 \pm 0.14$ K. Similar to Pb, data above T_2 is seen to follow a linear trend but is not used to estimate T_c as this trend is seen to break for the recorded value at T_2.

Unlike Pb, Figure 4 implies the resistivity of NbTi experiences an extremely sudden decrease in resistivity near T_c, rather than a gradual decrease before reaching 0 Ω·m. Though the data for temperatures just above T_2 is sparse, this distinction can still be clearly observed.

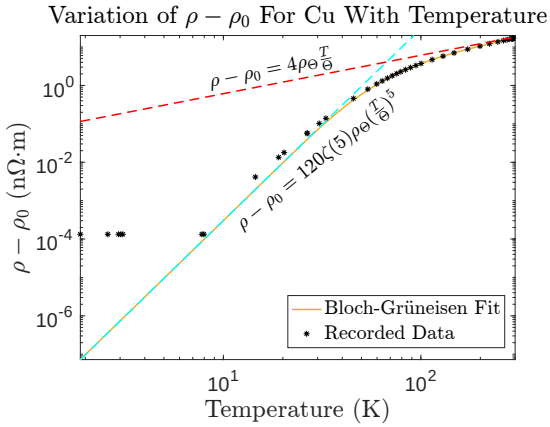

FIG. 5: Measured resistivity of Copper as a function of temperature compared to a Bloch–Grüneisen fit. The residual resisitivity is removed to highlight the difference in the slope of the data over the range of temperatures. Parameters of the fit are given by $\Theta = 316$ K, $\rho_\Theta = 19.3$ nΩ·m, and $\rho_0 = 0.135$ nΩ·m. At very low temperatures the curves do not match due to noise present in the measured values.

The Cu sample, unlike the Pb and NbTi samples did not experience a transition to superconductivity: Measurements below 3.01 K were seen to result in a resistivity of either 0.135 nΩ · m or 0.134 nΩ · m, resulting in the

sudden divergence of the two curves at lower temperatures. This can likely be attributed to noise or a lack of precision in the recording instruments.

The recorded data in Figure 5 nearly exactly fit the Bloch–Grüneisen model. The relationship $\rho \propto T^5$ is also clearly seen at lower temperatures, and $\rho \propto T$ is seen to begin near higher temperatures. The reason the trend $\rho \propto T$ is not seen as clearly as the $\rho \propto T^5$ trend can be explained by the recorded temperatures being below Θ, after which this trend is expected to be most accurate.

Similarly to Cu, Dy was also not seen to exhibit superconductivity. Unlike the material previously discussed,

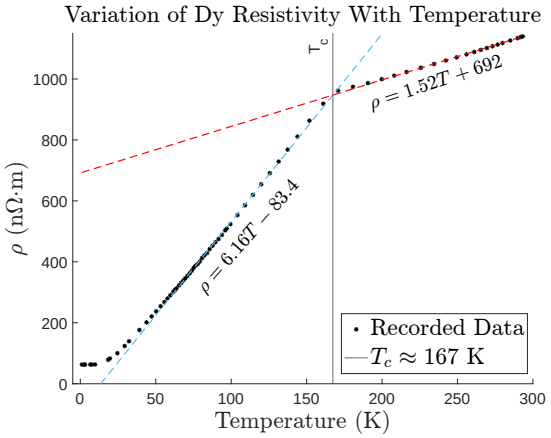

FIG. 6: Plot of calculated Dy resistivity. The change in slope near the magnetic ordering temperature (T_c) is highlighted by the dashed blue and red lines, giving a linear fit using the measurements for lower, and higher temperatures respectively. The units in the equations describing the trend line have units that are implied to match those presented on the axes. Pb's ρ_0 is measured to be 62.7 Ω·m.

Dy is seen to have a drastically different behavior in its resistivity profile at higher temperatures. At around 167 K, the slope of the trend line followed by the resistivity is seen to suddenly change from around 6.16 $\frac{\text{n}\Omega\cdot\text{m}}{\text{K}}$ for $T < T_c$ to 1.52 $\frac{\text{n}\Omega\cdot\text{m}}{\text{K}}$ for $T > T_c$. This break is attributed to a phase change in Dy that occurs around this temperature, in which the material transitions from being paramagnetic ($T > T_c$) to antiferromagnetic ($T < T_c$).

Due to abundant sampling at lower temperatures and temperatures near room temperature, the RRR can easily be calculated for Dy and Cu. The RRR for NbTi can also be approximated, with the assumption that the flatness seen in the Figure 4 for measurements at $T > T_2$ holds until the transition to superconductivty begins. Since the resistivity of Pb decreases uniformly to 0 Ω·m above T_2 (seen in Figure 3), a meaningful RRR cannot be assigned.

One major source of error in this experiment was the calibration of the thermometer. The initial review of the collected data showed that at room temperature, a voltage of 4.926 mV—implying a resistance of 49.26 Ω under a 100 mA current—corresponding to a temperature of around 278 K based off the manufacturer calibration settings, which also predicted a measured resistance of 47.43 Ω around 293.0 K. This was corrected for by scaling the measured resistance by a factor of 0.9665. It is very unlikely that is an accurate way to approach recalibrating the data, and it is likely that the deviations were nonlinear and not possible to accurately model based solely off the data collected in this experiment.

Material	ρ_0 (nΩ · m)	ρ_{293} (nΩ · m)	RRR
NbTi	298	356	1.19 ± 0.14
Cu	0.135	17.0	126 ± 22
Dy	62.7	1.13×10^3	18.8 ± 3.3

TABLE III: Computed values of ρ_0, ρ_{293}, and RRR corresponding to the resistivity measured at the lowest achieved temperatures, 293 K, and the residual resistivity ratio, respectively. ρ_0 was used in place of the typical $\rho_{4.2}$ due to the fact that $\rho \approx \rho_0$ for these samples at all temperatures recorded below 4.2 K.

Further, due to a lack of data as a result of equipment malfunction, there is very sparse data in temperature ranges of interest. There is a gap between temperatures of around 3.71 K and 6.62 K, as well as 9.74 K and 18.5 K (these ranges varied slightly between materials due to a short delay between measurements), which made accurate determination of T_c for Pb impossible. While recorded values for NbTi resistivity luckily allowed for a more precise interval in which T_c could be found, it omits data just before the transition, which would have allowed for a more thorough analysis of the transition to superconductivity.

CONCLUSION

In this experiment several low temperature phenomena were observed in NbTi, Pb, Cu, and Dy. Although some values (such as the transition temperature of Pb) were not able to be computed very accurately due to experimental mishaps, the recorded data shows clear transitions of NbTi and Pb to superconductivity, the transition of the resistivity of Cu from $\propto T^5$ to $\propto T$, and a clear phase transition of Dy corresponding to magnetic ordering.

The measured transition temperatures for NbTi and Pb differ slightly from recorded values. NbTi is known to have a transition temperature of ≈ 9.2 K, differing from the range of $T_c = 8.22 \pm 0.14$ K found in this experiment [1]. Pb is known to have a transition temperature of ≈ 7.18 K, which differs from the range $T_c = 13.2 \pm 4.5$ K found in this experiment [2]. These deviations are most likely attributed to the improper calibration of the thermometer, as previously discussed.

Likely due to similar issues responsible for the deviation of T_c measured in this experiment from standard values, the magnetic ordering temperature of Dy, found to be 167 K, is slightly different than the known transition temperature of 179 K [4]. Neutral Dy also has a recorded ρ_0 of 24 nΩm, which differs significantly from the $\rho_0 = 62.7 \pm 6.3$ measured in this experiment. However, another reference lists the RRR of Dy as 17.5 [9], falling within the measured RRR of 18.8 ± 3.3 in this experiment.

The material properties of copper vary greatly, particularly with the purity of the sample. One study found that different samples of copper can have RRR's ranging from 176 to 1018 [10]. Calatroni [11] also mentions that some Cu samples can have RRR's of 100, some of which are present in Apollonio et al. [12]. The Debye temperature can also be computed based on the speed of sound, c_s, in Cu, which gives a value of $\approx$ 343 K [6]. This is slightly different than the computed value of $\Theta = 316$ K.

Despite the differences of the measurements made in this experiment in comparison to data from scientific literature, the resistivity profiles of most solids are known to greatly depend on material characteristics such as sample purity, which can vary greatly sample to sample. Therefore, one cannot expect perfect alignment of all of these quantities between different samples. In addition, the the measurements in this experiment were on the same order of magnitude as the values in the literature which makes it reasonable to assume systematic error accounted for a large part of the deviation observed.

Clearly, the lack of properly calibrated temperature measurements is detrimental to an experiment of this nature. While the values obtained were surprisingly close to the values from the stated references, future renditions of the experiment would greatly benefit from thorough recalibration of the thermometer. Without confidence in the temperature measurements, it is impossible to verify the accuracy of the phase transition temperatures (for both superconductivity and magnetic ordering) for NbTi, Pb, and Dy (as well as the Debye temperature from fitting to the recorded Cu data).

Further, future experiments would also greatly benefit from collection of more data at low temperatures. This would highlight the transitions to superconductivity (especially for NbTi, due to the sparsity of data collected after T_2 seen in Figure 4). In order collect more data points to better view the phase transition and estimate the transition temperature, future experiments can lift the samples above the liquid helium bath to slowly warm the samples from ~ 4 K until the superconductors reach temperatures near their T_c. This would give much more data near temperatures that could not be measured and highlight the nature of the transitions, allowing for a more detailed discussion of some of the phenomena studied in this experiment.

[1] M. Lubell, IEEE Transactions on Magnetics **19**, 754 (1983).

[2] W. B. Pearson and I. M. Templeton, Phys. Rev. **109**, 1094 (1958), URL `https://link.aps.org/doi/10.1103/PhysRev.109.1094`.

[3] J. Ziman, *Electrons and Phonons: The Theory of Transport Phenomena in Solids* (NA, 2001), URL `https://api.semanticscholar.org/CorpusID:94493724`.

[4] M. K. Wilkinson, W. C. Koehler, E. O. Wollan, and J. W. Cable, J. Appl. Phys. **32**, S48 (1961).

[5] D. van Delft and P. Kes, Phys. Today **63**, 38 (2010).

[6] C. Kittel, *Introduction to Solid State Physics* (John Wiley and Sons, 1953).

[7] D. V. Baak, *Noise Fundamentals Instructors Manual* (2010).

[8] G. K. White and P. Meeson, *Experimental techniques in low-temperature physics*, Monographs on the Physics and Chemistry of Materials (Oxford University Press, London, England, 2001).

[9] V. I. Sokolenko, A. O. Chupikov, M. M. Pylypenko, M. B. Lazareva, and O. Y. Roskoshna, Low Temp. Phys. **50**, 125 (2024).

[10] A. Vorobieva, A. Nikulin, A. Shikov, V. Pantsyrny, M. Polikarpova, N. Kozlenkova, E. Dergunova, E. Popova, and L. Rodionova, Physica C Supercond. **354**, 371 (2001).

[11] S. Calatroni, *Materials & properties: Thermal & electrical characteristics* (2020), 2006.02842, URL `https://arxiv.org/abs/2006.02842`.

[12] A. Apollonio, R. Schmidt, A. Verweij, M. Solfaroli, and M. Koratzinos (2012).